






Research Article

MHD Stagnation Point Radiative Flow of Hybrid Casson Nanofluid Across a Stretching Surface

Sandhya Rani¹, Venkata Ramana Reddy¹, W Sridhar¹, Ali Akgül^{2,3}, Abdulrhman M Alsharari⁴, Jihad Asad^{5*}

¹Department of Engineering Mathematics, Koneru Lakshmaiah Education Foundation, Vaddeswaram 522302, India

²Department of Mathematics, Faculty of Art and Science, Siirt University, Siirt 56100, Turkey

³Department of Electronics and Communication Engineering, Saveetha School of Engineering, SIMATS, Chennai 602105, Tamilnadu, India

⁴Department of Physics, University of Tabuk, Tabuk 71491, Saudi Arabia

⁵Department of Physics, Faculty of Applied Science, Palestine Technical University-Kadoorie, Tulkarm P 305, Palestine
E-mail: j.asad@ptuk.edu.ps

Received: 31 March 2023; **Revised:** 13 June 2023; **Accepted:** 31 July 2023

Abstract: The current investigation explores the hybrid Casson nanofluid stagnation point flow on a transient stretching surface under the impact of thermal radiation. The Joule heating effect is also considered in this study. Copper and aluminium hybrid nanoparticles are used. The guiding partial differential equations are broken down into nonlinear ordinary differential equations using adequate affinity transmutations. The subsequent equations are worked out by employing the Keller box scheme. The numerical findings for the study are represented by plotting velocity, and temperature graphs for various parameters like radiation parameter (Rd), Casson parameter (β), magnetic parameter (M), Prandtl number (Pr), and unsteady parameter (s). As well, the local parameters coefficient of skin friction is calculated. For progressive estimates of the Casson parameter, the velocity of the liquid flow reduces. On intensifying the Prandtl number temperature of the fluid diminishes. Also, the effect of nanoparticles volume fraction of both nanoparticles is observed. It was found that for escalating values of both nanoparticle velocities, the velocity of the fluid flow reduces and the opposite trend is observed for the temperature profile. The usage of hybrid nanofluids has the advantage of heat transfer enhancement. The outcomes of the current investigation are good and in congruence with existing literature.

Keywords: casson fluid, hybrid nanofluid, MHD, radiation, keller box method

MSC: 76W05, 80A19

Nomenclature

β	Casson Parameter
M	Magnetic field parameter
Pr	Prandtl number

Ec	Eckert number
S	stretching parameter
ϕ_1	nanoparticle volume fraction
ϕ_2	hybrid Nano fluid volume fraction
ρ_{nf}	Nanofluid density
ρ_{hnf}	density of hybrid nanofluid
k_{nf}	thermal conductivity of nanofluid
σ	electrical conductivity

1. Introduction

Nanofluids are novel fluids constructed by dissolving nanometer-sized components such as nanosheets, nanotubes, and nanofibers in base fluids. In another manner, nanofluids are nanoscale colloidal solutions that include condensed nanosubstances. Nanofluids have improved thermo physical characteristics and convective heat transfer coefficient, similar to viscosity, thermal diffusivity and thermal conductivity when compared to base fluids like water or oil. It offers a wide range of possible uses in a variety of sectors in heat transfer applications such as industrial cooling systems, nuclear reactors, automotive applications such as coolants, electronic applications such as cooling of microchips, biomedical applications such as nano drug delivery, cancer therapy, nanosurgery, sensing and imaging (Yu et al. [1], Wong et al. [2]).

From the previous works, it is noted that in a few cases of nanofluid, it was witnessed that specific heat is very low when compared to base fluid, also thermo physical properties of nanofluid depend on the dimensions of the nanomaterials used. Due to some lack of clarity in nanofluids, a new type of fluid is created by suspending various nanoparticles as a mixture or as a composite form called hybrid nanofluids. Hybrid nanofluids represent a novel class of fluids prepared as per blend of non-metallic or metallic nano-contented particles with base fluid acquainted to develop heat transfer rate when compared with base fluids. As demonstrated by several applications in cooling systems, heat turbines in industries, heat generators, drug delivery, and biological problems caused by nanofluids, this class of nanofluid model effectively enhances heat transfer phenomena. The goal of integrating two distinct nanoparticles will augment thermal conductivity. These liquids have distinct implementations in the medical sciences field, most medications are generated in the form of hybrid nanofluids, and blood is utilized as base fluid to monitor the chemical reactions of components in the blood. To the improvement of the thermal properties of such liquid, nanoparticles dispersed in the base fluid will enhance thermo physical properties. In the present paper a two-dimensional boundary layer flow of a heat transfer non-Newtonian Casson hybrid Nanofluid ($Al_2 + Cu + Water$) across a stretched surface as its stagnation point is considered. Choi et al. [3] investigated that by delaying metallic nano particulates trendy base fluid resulting fluid exhibit higher thermal conductivity and advancement in heat transfer was observed. Also, practical applications of Nanofluid are analyzed by Dash et al. [4] intended Casson liquid flow in porous pipe and observed that increasing yield stress of fluid decrease in permeability is observed. Later Lee et al. [5]. Empirically measured about thermal conduction of nanofluid. After that Xuan et al. [6] studied heat transfer improvement in the nanofluids case and observed that suspending nanoparticles increases thermal conductivity. Mernone et al. [7] analyzed the peristaltic transport of Casson fluid using the perturbation series method. Later Hong et al. [8] studied Fe nano liquids and observed that the thermal conductivity of the nanofluid rises, and the volume fraction of nanoparticles improves. Later Khan et al. [9] analyzed Nanofluid flow on a stretched sheet for higher values of Pr, Sherwood number increases. Warriar et al. [10] discussed that particle size will affect the enhancement of the thermal conduction of Nano liquid. Saidur et al. [11] reviewed the applications of nanofluids. After that, Suresh et al. [12] experimentally studied Cu- Al_2O_3 - H_2O hybrid nano-liquid flow and observed that the heat transfer coefficient increases with increasing Reynolds number. Bhattacharyya [13] studied "Boundary layer stagnation-point flow of Casson fluid and heat transfer towards a shrinking/stretching sheet. Haq et al. [14] studied Convective heat transfer and MHD effects on Casson Nanofluid flow over a shrinking sheet. Mansur et al. [15] studied boundary layer Nanofluid flow over a stretched sheet utilizing the shooting method; observed the hat heat transfer rate reduced with higher numerals of unsteadiness factor. Later Esfe et al. [16] aimed experimentally about the conductivity and viscosity of hybrid nanofluid and observed that increasing the thermal conductivity of nanoparticles and dynamic fluid viscosity enhances. Later Harandi et al. [17] studied f-MWCNT

Fe₃O₄-EG hybrid nano liquids' thermal conductivity; noted thereto thermal conductivity enhances, an increase in solid volume fraction and temperature. Thereafter, Hymavathi et al. [18] studied Casson MHD liquid flow using the Keller box method; observed that an increase in Schmidt number causes a decrease in concentration profiles. Later Ibrahim et al. [19] studied Nano fluid Casson flow over a stretched sheet using RK-Fehlberg; observed that Sherwood decreases with a rise in the Casson parameter. Later Devi et al. [20] studied cu-Al₂O₃ hybrid nano liquid flow across a stretched sheet; hence the conclusion is the usage of hybrid nanofluid under magnetic field heat transfer rate enhances. Esfe et al. [21] analyzed about thermal conduction of SWCNT-MgO hybrid nanofluid. Ghadikolaei et al. [22] studied MHD Nano liquid Casson flow as well as radiation impact across an inclined stretched sheet RK Fehlberg method; hence the conclusion is increasing radiation parameter heat transfer rate increases. Later Aman et al. [23] presented an influence of the magnetic field flow of a Casson hybrid Nano liquid using the Laplace transform technique. Later Sajid et al. [24] reviewed the thermal conductivity of nanofluids. Akhgar et al. [25] studied H₂O-ethylene glycol, SWCNT- TiO₂ hybrid nano liquid flow, which was seen to rise as the temperature and volume fraction of the Nanofluid raised. Balaji et al. [26] reviewed the radiation impact of MHD Casson Nano liquid on the vertical plate and solved using the closed analytical method velocity of fluid falls with an increment in radiation. Narender et al. [27] explored the flow of stagnation point a Casson nanofluid flow on the radially stretched sheet using the shooting technique; for higher values of Prandtl number, temperature falls were concluded. After that Sridhar et al. [28] explored combined convective Casson fluid flow on an inclined stretched sheet; the increase in permeability parameter velocity decreases. Later Krishna et al. [29] studied Casson hybrid nanofluid using the Laplace transform technique; the Nusselt number rises with increment in heat absorption rate. After that Sridhar et al. [30] studied the MHD flow of Casson fluid across a stretched surface; an increasing radiation parameter will enhance the temperature. Wang [31], Free convection on a vertical stretching surface, Thereafter, Ganesh et al. [32] studied MHD Casson fluid through Darcy for chimer porous media and observed that for progressive values of magnetic velocity decreases. Agamid et al. [33] reported Casson-Cu+Al₂ hybrid Nanofluid; an increase in Casson factor velocity of the fluid declines. Xu et al. [34, 35] investigates gas passage behaviour in nanopores and discussed that the packing fraction of the gas equation of state offers the smallest limits for the Knudsen number and flow system. Also, with a Knudsen number and a pore diameter, one can easily estimate the apparent permeability of gas for flow-regime conditions from a typical gas apparent permeability curve. Atashafrooz [36] studied hybrid nanofluid flow inside a trapezoidal enclosure with the influence of radiative heat transfer and magnetic field and concluded that in the absence of a magnetic field highest magnitude of heat transfer rate is obtained at the bottom of the enclosure. Sajjadi et al. [37] investigated the influence of magnetic field on particle suspension in a modelled room and concludes that for higher values of magnetic field influence the number of suspended particles on the walls increases also gravity force has a notable influence on particle suspension and their presence on the floor of the modelled room. Delouei et al. [38] investigated experimentally the influence of concentration of the nanofluid on ultrasonic vibrating finned tube heat exchanger and noted that increasing concentration of the nanofluid will influence ultrasonic vibration effect. Also decreasing the surrounding temperature and velocity of the air heat transfer enhances and the positive impact of ultrasonic vibrations decreases.

2. Formulation of the problem

In the Current investigation, an incompressible, unsteady, two-dimensional stagnation point MHD boundary layer flow of non-Newtonian hybrid Nano liquid over a stretched surface with an impact of radiation is considered. From the Figure 1, the rheological equation of the Casson flow model is

$$\tau_{ij} = \begin{cases} 2(\mu_B + (2\pi)^{-\frac{1}{2}} p_y) e_{ij}, & \pi > \pi_c \\ 2(\mu_B + (2\pi)^{-\frac{1}{2}} p_y) e_{ij}, & \pi < \pi_c \end{cases}.$$

Here μ_B represents plastic dynamic viscosity, p_y represents yield stress.

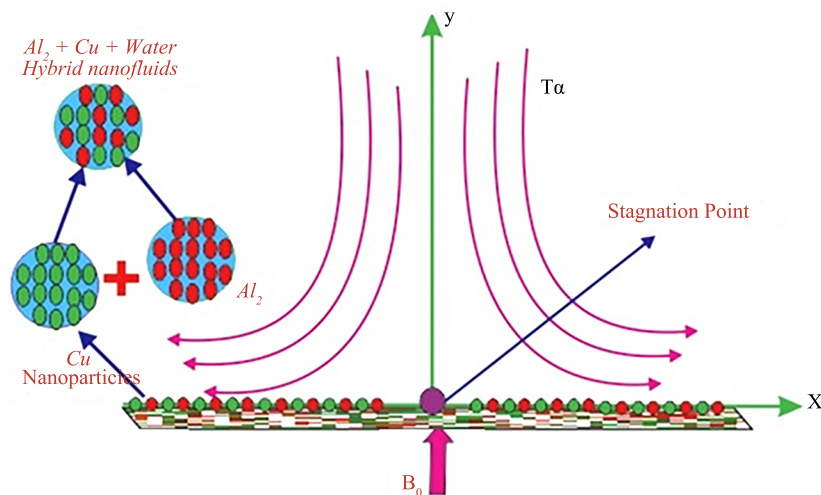


Figure 1. Physical geometry of the Problem

Under these assumptions, the governing flow partial differential equations are:

$$\frac{\partial u}{\partial x} + \frac{\partial v}{\partial y} = 0 \quad (1)$$

$$\frac{\partial u}{\partial t} + u \frac{\partial u}{\partial x} + v \frac{\partial u}{\partial y} = \frac{dU_s}{dt} + U_s \frac{dU_s}{dx} + \nu_{hnf} \left(1 + \frac{1}{\beta} \right) \frac{\partial^2 u}{\partial y^2} + \frac{\sigma_{hnf} B_0^2}{\rho_{hnf}} (U_s - u) \quad (2)$$

$$\frac{\partial T}{\partial t} + u \frac{\partial T}{\partial x} + v \frac{\partial T}{\partial y} = \left(\frac{k}{\rho c_p} \right)_{hnf} \frac{\partial^2 T}{\partial y^2} - \left(\frac{1}{\rho c_p} \right)_{hnf} \frac{\partial q_r}{\partial y} + \frac{\sigma_{hnf} B_0^2}{(\rho c_p)_{hnf}} (U_s - u)^2 \quad (3)$$

where u and v represents velocity components in the x and y directions. k represents thermal conductivity. c_p represents specific heat. ρ represents fluid density. U_s represents stagnation point flow velocity. ν represents kinematic viscosity.

Relative boundary conditions:

$$u = U_w, v = 0, T = T_w \text{ at } y = 0 \text{ and } u \rightarrow U_s, T \rightarrow T_\infty \text{ as } y \rightarrow \infty. \quad (4)$$

Using the similarity transformations

$$\eta = \sqrt{\frac{a}{(1-\alpha t)\nu_f}} y, \psi = \sqrt{\frac{a}{1-\alpha t}} \nu_f x f(\eta), \theta = \frac{T - T_\infty}{T_w - T_\infty}$$

the equation (1) which represents the equation of continuity is satisfied by using the relations $u = \frac{\partial \psi}{\partial y}$, $v = -\frac{\partial \psi}{\partial x}$.

Equations (2)-(3) are transformed to

$$\left(1 + \frac{1}{\beta}\right) f''' + (1 - \phi_1)^{2.5} (1 - \phi_2)^{2.5} \left[(1 - \phi_2) \left[1 - \phi_1 + \phi_1 \frac{\rho_{s1}}{\rho_f} \right] + \phi_2 \frac{\rho_{s2}}{\rho_f} \right] \quad (5)$$

$$\left[-f'^2 + f f'' - S \left[f' + \frac{\eta}{2} f'' \right] \right] + M [1 - f'] = 0$$

$$\frac{k_{hmf}}{k_{bf}} \left(1 + \frac{4}{3} Rd \right) \theta'' - \left[\left[1 - \phi_1 + \phi_1 \frac{(\rho c_p)_{s1}}{(\rho c_p)_f} \right] (1 - \phi_2) + \frac{(\rho c_p)_{s2}}{(\rho c_p)_f} \phi_2 \right] \left[\text{Pr} \left(f \theta' + \frac{S}{2} \eta \theta' + EcM(f' - 1)^2 \right) \right] = 0 \quad (6)$$

Boundary conditions in (4) are transformed to the form

$$f(0) = 0, f'(0) = \frac{c}{a}, \theta(0) = 1 \quad (7)$$

$$f'(\infty) \rightarrow 1, \theta(\infty) \rightarrow 0$$

3. Method of solution

Equations (5)-(6) along with given BCs are resolved using the Keller box scheme as reported by Cebecci and Bradshaw (33) the steps to follows:

1. Deduce the specified system into 1st order non-linear equation.
2. Employ finite difference and then linearized.
3. Deduce the specified system to a tridiagonal system.
4. Using block tridiagonal elimination we solve the tri-diagonal system.

Using the above process the linear equations system we get are

$$\delta f_j - \delta f_{j-1} - \frac{h_j}{2} (\delta p_j + \delta p_{j-1}) = (r_1)_j \quad (8)$$

$$\delta p_j - \delta p_{j-1} - \frac{h_j}{2} (\delta q_j + \delta q_{j-1}) = (r_2)_j \quad (9)$$

$$\delta g_j - \delta g_{j-1} - \frac{h_j}{2} (\delta t_j + \delta t_{j-1}) = (r_3)_j \quad (10)$$

$$(a_1)_j \delta q_j + (a_2)_j \delta q_{j-1} + (a_3)_j \delta p_j + (a_4)_j \delta p_{j-1} + (a_5)_j \delta f_j + (a_6)_j \delta f_{j-1} = (r_4)_j \quad (11)$$

$$(b_1)_j \delta t_j + (b_2)_j \delta t_{j-1} + (b_3)_j \delta f_j + (b_4)_j \delta f_{j-1} + (b_5)_j \delta p_j + (b_6)_j \delta p_{j-1} = (r_5)_j \quad (12)$$

where

$$(r_1)_j = f_{j-1} - f_j + \frac{h_j}{2} (p_j + p_{j-1}) \quad (13)$$

$$(r_2)_j = p_{j-1} - p_j + \frac{h_j}{2} (q_j + q_{j-1}) \quad (14)$$

$$(r_3)_j = g_{j-1} - g_j + \frac{h_j}{2} (t_j + t_{j-1}) \quad (15)$$

$$(r_4)_j = q_{j-1} - q_j + \left(\frac{\beta h_j}{4(\beta+1)} (p_j + p_{j-1})^2 - \frac{\beta h_j}{4(\beta+1)} (f_j + f_{j-1}) (q_j + q_{j-1}) + \frac{S\beta}{2(\beta+1)} (p_j + p_{j-1}) + \frac{S\eta\beta}{4(\beta+1)} (q_j + q_{j-1}) \right) \\ ((1-\phi_1)^{3.5} (1-\phi_2)^{3.5} + (2.7181)\phi_1 (1-\phi_1)^{2.5} (1-\phi_2)^{2.5} + (8.9869)\phi_2 (1-\phi_1)^{2.5} (1-\phi_2)^{2.5} \\ - \frac{M\beta h_j}{\beta+1} + \frac{M\beta h_j}{2(\beta+1)} (p_j + p_{j-1}) \quad (16)$$

$$(r_5)_j = t_{j-1} - t_j + \left(\frac{-\frac{3Prh_j}{4(3+4Rd)} (f_j + f_{j-1}) (t_j + t_{j-1}) - \frac{3Prh_j S\eta}{4(3+4Rd)} (t_j + t_{j-1}) - \frac{3Prh_j EcM(p_j+p_{j-1})^2}{4(3+4Rd)} + \frac{3Prh_j EcM(p_j+p_{j-1})}{4(3+4Rd)} - \frac{3Prh_j EcM}{4(3+4Rd)} \right) \\ ((1-\phi_1)(1-\phi_2)(0.8399) + \phi_1(1-\phi_2)(0.4915) + \phi_2(0.7024)) \quad (17)$$

$$(a_1)_j = 1 + \left(\frac{\beta h_j}{4(\beta+1)} (f_j + f_{j-1}) - \frac{S\eta\beta}{4(\beta+1)} \right) \\ ((1-\phi_1)^{3.5} (1-\phi_2)^{3.5} + (2.7181)\phi_1 (1-\phi_1)^{2.5} (1-\phi_2)^{2.5} + (8.9869)\phi_2 (1-\phi_1)^{2.5} (1-\phi_2)^{2.5} \quad (18)$$

$$(a_2)_j = (a_1)_j - 2.0 \quad (19)$$

$$(a_3)_j = \left(-\frac{\beta h_j}{2(\beta+1)} (p_j + p_{j-1}) - \frac{S\beta}{2(\beta+1)} \right) \\ ((1-\phi_1)^{3.5} (1-\phi_2)^{3.5} + (2.7181)\phi_1 (1-\phi_1)^{2.5} (1-\phi_2)^{2.5} + (8.9869)\phi_2 (1-\phi_1)^{2.5} (1-\phi_2)^{2.5} \quad (20)$$

$$(a_4)_j = (a_3)_j \quad (21)$$

$$(a_5)_j = \frac{\beta h_j}{4(\beta+1)} (q_j + q_{j-1}) \\ ((1-\phi_1)^{3.5} (1-\phi_2)^{3.5} + (2.7181)\phi_1 (1-\phi_1)^{2.5} (1-\phi_2)^{2.5} + (8.9869)\phi_2 (1-\phi_1)^{2.5} (1-\phi_2)^{2.5} \quad (22)$$

$$(a_6)_j = (a_5)_j \quad (23)$$

$$(b_1)_j = \left[1 + \left(\frac{3\text{Pr}h_j}{4(3+4Rd)} + \frac{3\text{Pr}S\eta}{4(3+4Rd)} \right) \right] \left(\begin{array}{l} (1-\phi_1)(1-\phi_2)(0.8399) \\ +\phi_1(1-\phi_2)(0.4915) + \phi_2(0.7024) \end{array} \right) \quad (24)$$

$$(b_2)_j = (b_1)_j - 2.0 \quad (25)$$

$$(b_3)_j = \frac{3\text{Pr}h_j}{4(3+4Rd)} (t_j + t_{j-1}) ((1-\phi_1)(1-\phi_2)(0.8399) + \phi_1(1-\phi_2)(0.4915) + \phi_2(0.7024)) \quad (26)$$

$$(b_4)_j = (b_3)_j \quad (27)$$

$$(b_5)_j = \left(\frac{3\text{Pr}EcMh_j}{2(3+4Rd)} (p_j + p_{j-1}) - \frac{3\text{Pr}EcMh_j}{2(3+4Rd)} \right) \left(\begin{array}{l} (1-\phi_1)(1-\phi_2)(0.8399) \\ +\phi_1(1-\phi_2)(0.4915) + \phi_2(0.7024) \end{array} \right) \quad (28)$$

$$(b_6)_j = (b_5)_j \quad (29)$$

The system of equations (8)-(12) become

$$[A_1][\delta_1] + [C_1][\delta_2] = [r_1]$$

$$[B_2][\delta_1] + [A_2][\delta_2] + [C_2][\delta_3] = [r_2]$$

$$[B_{j-1}][\delta_1] + [A_{j-1}][\delta_2] + [C_{j-1}][\delta_3] = r_{j-1}$$

$$[B_j][\delta_{j-1}] + [A_j][\delta_j] = [r_j]$$

(30)

where,

$$A_1 = \begin{bmatrix} 0 & 0 & 1 & 0 & 0 \\ d & 0 & 0 & d & 0 \\ 0 & d & 0 & 0 & d \\ (a_2)_1 & 0 & (a_5)_1 & (a_1)_1 & 0 \\ 0 & (b_2)_1 & (b_3)_1 & 0 & (b_1)_1 \end{bmatrix} \quad A_j = \begin{bmatrix} d & 0 & 1 & 0 & 0 \\ -1 & 0 & 0 & d & 0 \\ 0 & -1 & 0 & 0 & d \\ (a_4)_2 & 0 & (a_5)_2 & (a_1)_2 & 0 \\ 0 & 0 & (b_3)_2 & 0 & (b_1)_2 \end{bmatrix}$$

$$B_j = \begin{bmatrix} 0 & 0 & -1 & 0 & 0 \\ 0 & 0 & 0 & d & 0 \\ 0 & 0 & 0 & 0 & d \\ 0 & 0 & (a_6)_2 & (a_2)_2 & 0 \\ (b_6)_2 & 0 & (b_4)_2 & 0 & (b_2)_2 \end{bmatrix} \quad C_j = \begin{bmatrix} d & 0 & 0 & 0 & 0 \\ 1 & 0 & 0 & 0 & 0 \\ 0 & 1 & 0 & 0 & 0 \\ (a_3)_j & 0 & 0 & 0 & 0 \\ (b_5)_j & 0 & 0 & 0 & 0 \end{bmatrix}$$

Here $j = 1, 2, 3, \dots, n - 1$.

Subsequent equations were solved using the LU decomposition method. The calculating procedure should be halted until it meets the convergence criterion. The determinations are concluded for $|\delta g_0^{(i)}| < \varepsilon$, $\varepsilon = 0.00001$.

4. Results and discussion

A stagnation point flow of Casson hybrid nanofluid on a stretching surface is considered. The flow is influenced by the applied magnetic field and Joule heating influences. Hybrid nanofluid is prepared by suspending nanoparticles of Copper (Cu) and Aluminium (Al_2) in the base fluid. The equations governing the flow model are solved using the Keller Box method. The flow is influenced by non-dimensional parameters Casson (β), Magnetic (M), nanoparticle volume fraction (ϕ_1, ϕ_2), unsteady parameter (S) Prandtl number (Pr), Radiation parameter (Rd), Eckert number (Ec). The Impact of these parameters is observed by scheming temperature and velocity profiles utilizing MATLAB. The Nusselt number is calculated for progressive values of the Prandtl number it is found that on increasing Prandtl number enhancement in Nusselt number is witnesses this phenomenon coincides with previous literature mentioned in Table 1. Also, the numerical calculation of local parameters skin friction coefficient was calculated and observed, skin friction value rises for greater values of Casson parameter, Magnetic parameter depicted in Table 2 and incorporated thermal physical properties of the fluid nano particles in Table 3.

Table 1. Comparison study of $-\theta'(0)$

Pr	Khan & Pop [9]	Wong [2]	Anjali devi & Uma devi [20]	Present study
7	1.8954	1.8954	1.8954	1.8956
20	3.3539	3.3539	3.3539	3.3289
70	6.4621	6.4622	-	6.3842

Table 2. Skin friction coefficient values for β and M

B	M	$f''(0)$, Cu+ Casson	$f''(0)$, Cu+Casson+ Al_2
0.3	0.6	0.3724	0.2340
0.5		0.4557	0.2620
0.7	0.7	0.5520	0.2880
	0.8	0.5915	0.2934
	0.9	0.6469	0.2989

Table 3. Thermo-physical of fluid and nanoparticles

Property	Water	Al_2	Cu
Density	997	2710	8960
Specific heat	4180	900	389
Thermal conductivity	0.6071	205	398
Electrical conductivity	5.5×10^{-6}	3.5×10^7	59.6×10^6

An impact effect of the Casson parameter in velocity characterization is portrayed in Figure 2 both Casson+Cu fluid and Casson+Al₂+Cu hybrid nanofluid. Clearly, for progressive values of Casson parameter velocity declines. An improving Casson factor value fluid elasticity of hybrid fluid increases, so the viscosity of the hybrid nanofluid increases. Figure 3 displays velocity profiles of Magnetic parameter. On improving magnetic parameters, fluid velocity lessens in both cases of nanofluid as well as hybrid nanofluid due to the opposing force generated called Lorentz force. Figure 4 represents velocity profiles corresponding to nanoparticle volume friction factors ϕ_1 , ϕ_2 . Improving values of ϕ_1 , ϕ_2 velocity profiles exhibits decreasing tendency for both Casson nano and Casson hybrid nanofluids. Because rising values of ϕ_2 cause a reduction in the thickness of the moment boundary layer. Velocity profiles of the unsteady parameter are portrayed in Figure 5. On increasing the unsteady parameter, the velocity of the fluid decreases owing to improving values on the unsteady parameter it generates a resistive force. Figure 6 demonstrates the temperature profiles of the Casson parameter. Casson factor progressive values on the temperature of the fluid increase. The fluid temperature rises for greater values of the Magnetic factor which is displayed in Figure 7. Figure 8 represents the temperature distribution of the Prandtl number. With higher values of Prandtl number, the decreasing trend is observed in temperature profiles for both Casson nano and hybrid nanofluids cases due to the reason for higher values of Prandtl number, thermal conduction of fluid lessens. Temperature profiles of radiation parameter are portrayed in Figure 9. For higher values of radiation factor, the temperature of fluid increases because on increasing thermal radiation parameter TBL thickness decreases more heat will be generated so temperature profile increases. Figure 10 displays temperature profiles for nanoparticle volume friction parameters. It is visible that the increase in values of ϕ_1 , ϕ_2 temperature of the fluid increases for both Casson nano and Casson and nanofluid cases. Figure 11 portrays the temperature profile for various values of the Eckert number. It was noticed, temperature turned out to increase for progressive values of Eckert number. Eckert number arises from the application of the Joule heating effect along with the magnetic field. An Increase in Eckert number drives a rise in kinetic energies resulting increase in the collision of fluid molecules causing a rise in the temperature profile.

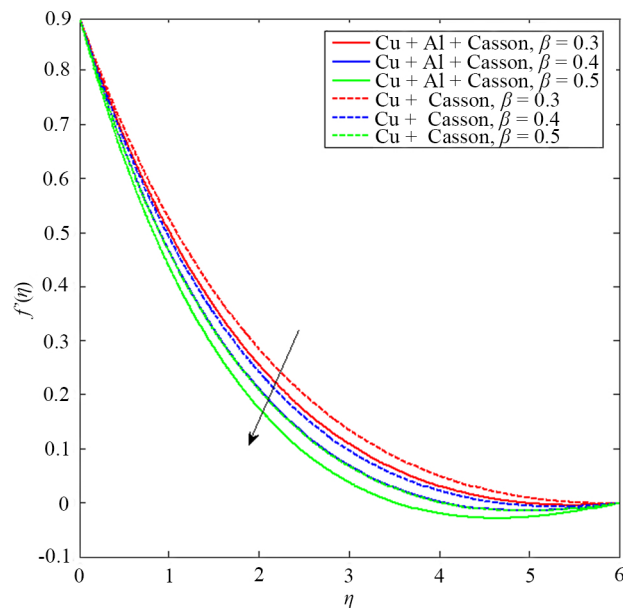


Figure 2. Velocity characterization of β

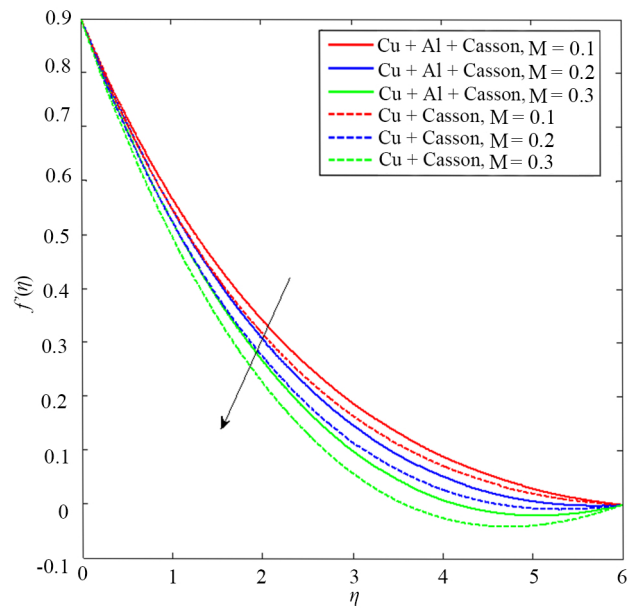


Figure 3. Velocity characterization of M

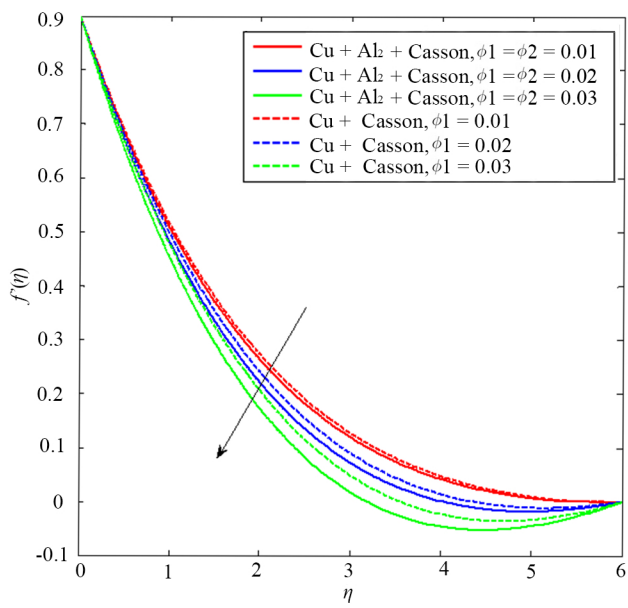


Figure 4. Velocity characterization for nanoparticle volume fraction

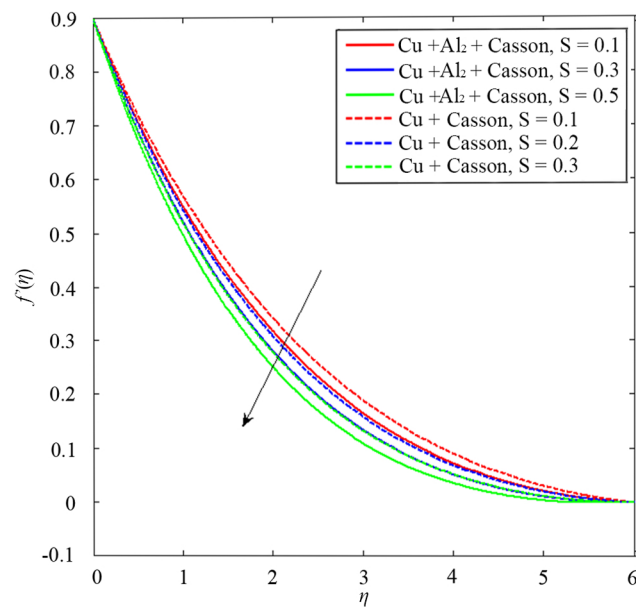


Figure 5. Velocity characterization of unsteady parameter S

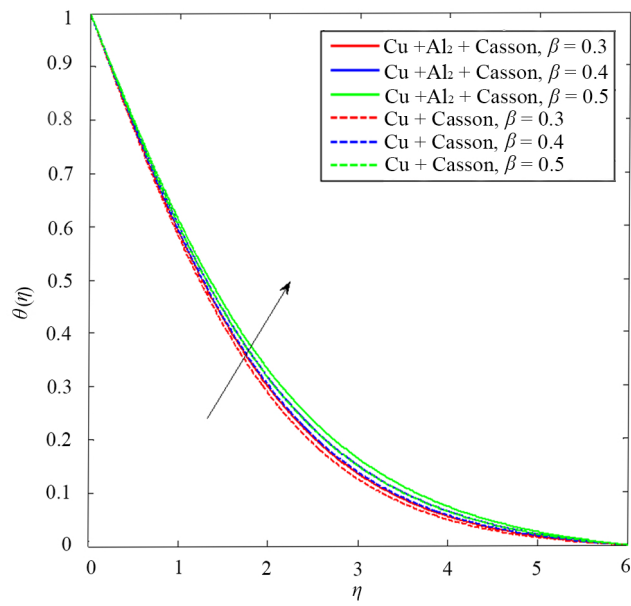


Figure 6. Temperature characterization of Casson parameter β

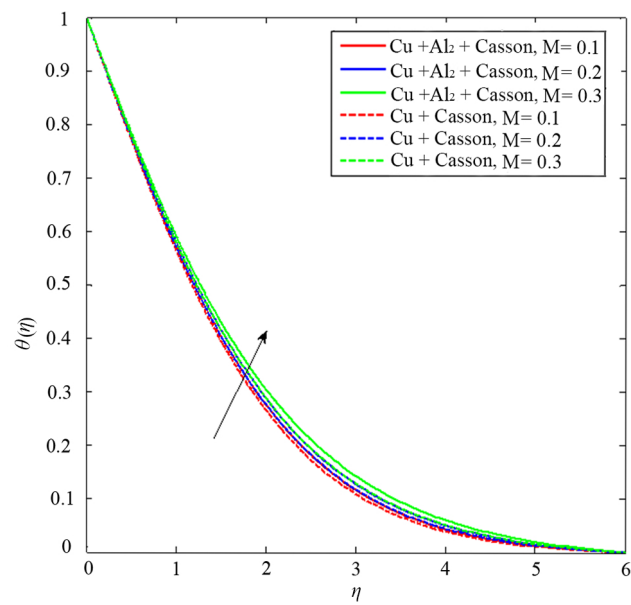


Figure 7. Temperature characterization of Magnetic parameter M

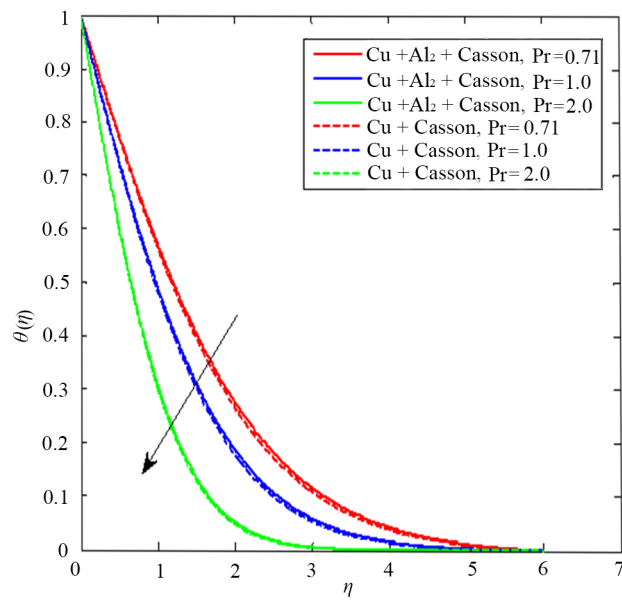


Figure 8. Temperature characterization of Prandtl number Pr

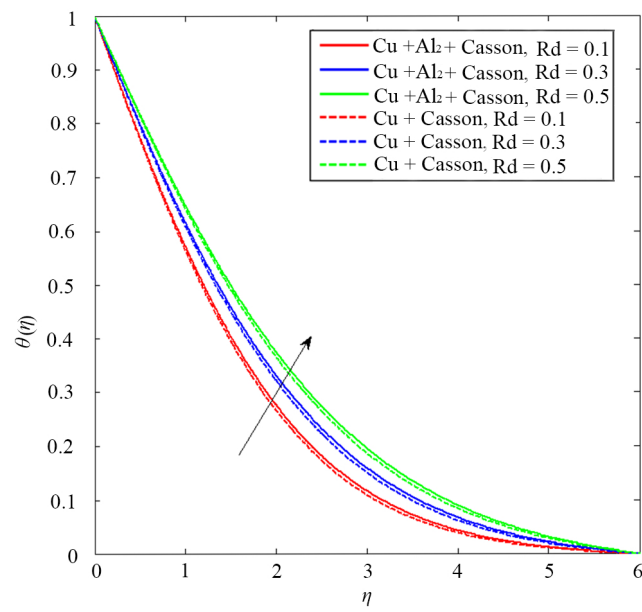


Figure 9. Temperature characterization of Radiation parameter R_d

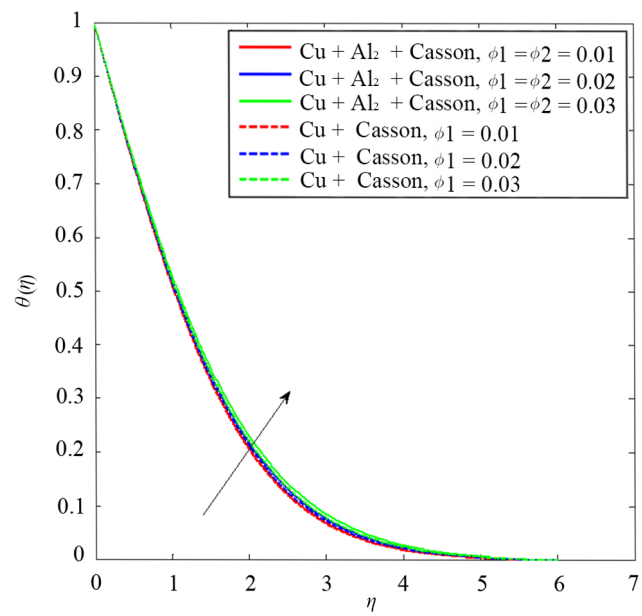


Figure 10. Temperature characterization of Nanoparticle

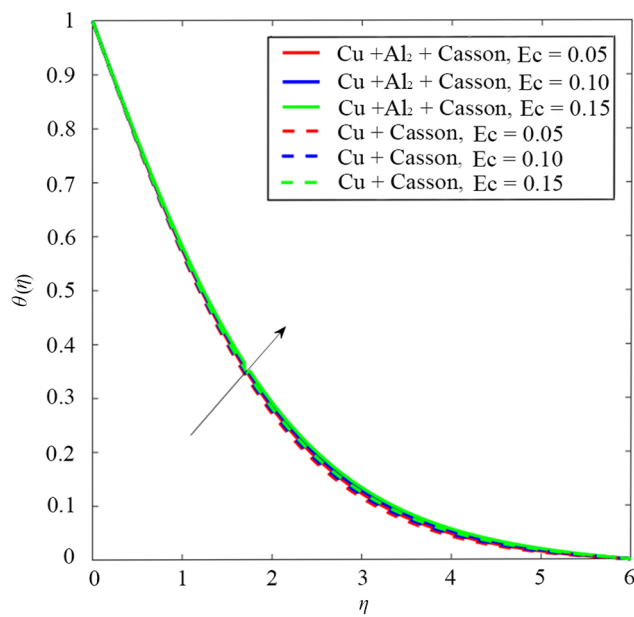


Figure 11. Temperature profiles for Eckert number volume fraction

To validate the numerical method, present results are compared with existing literature by calculating $-\theta'(0)$ taking $\phi_1 = \phi_2 = 0$. By observing the Table 1, the results are found to be good in agreement with the existing literature. Increasing the Prandtl number, the Nusselt number increases.

Also, Numerical observations of the skin friction coefficient were calculated and observed that C_f -value.

Improves for greater values of Casson parameter, and Magnetic parameter.

5. Conclusions

In the present study, Casson hybrid nanofluid flow over a stretching surface is considered with the MHD, Radiation and Joule heating influences. The study is carried out by solving the governing equations using the Keller Box method. Also a comparative study between Cu-Casson and Cu+Al₂-Casson hybrid nanofluid Cases. Also, the impact of various parameters is analysed by constructing graphs of velocity and temperature comparison of nanofluid (Cu+caason) with hybrid nanofluid (Cu+Al₂+Casson) using MATLAB. Also, numerical values of local parameters skin friction coefficient and Nusselt number are calculated. The following findings are observed.

- Greater values of Casson parameter, declination is observed in velocity profile and increasing trend is observed in temperature profiles.
- Stronger magnetic parameter impact, fluid velocity reduces, and fluid temperature rises.
- An improving value of nanoparticle volume friction factors ϕ_1 , ϕ_2 , fluid velocity enhancement, and fluid temperature reduces.
- An escalating value of Prandtl number, fluid temperature reduces.
- Progressive values of radiation factor, fluid temperature rises.
- Progressive values of Eckert number, increment in temperature profiles observed.

Acknowledgement

Jihad Asad would like to thank Palestine Technical University-Kadoorie for supporting this work financially.

Conflict of interest

The authors declare no competing financial interest.

References

- [1] Yu W, Xie H. A review on nanofluids: Preparation, stability mechanisms, and applications. *Journal of Nanomaterials*. 2012; 2012: 435873.
- [2] Wong KV, De Leon O. Applications of nanofluids: Current and future. *Nanotechnology and Energy*. 2017: 105-132.
- [3] Choi SU, Eastman JA. *Enhancing Thermal Conductivity of Fluids with Nanoparticles*. Argonne, IL, USA: Argonne National Lab. (ANL); 1995.
- [4] Dash RK, Mehta KN, Jayaraman G. Casson fluid flow in a pipe filled with a homogeneous porous medium. *International Journal of Engineering Science*. 1996; 34(10): 1145-1156.
- [5] Lee S, Choi SS, Li SA, Eastman JA. Measuring thermal conductivity of fluids containing oxide nanoparticles. *ASME* 1999; 121(2): 280-289.
- [6] Xuan Y, Li Q. Heat transfer enhancement of nanofluids. *International Journal of Heat and Fluid Flow*. 2000; 21(1): 58-64.
- [7] Mernone AV, Mazumdar JN, Lucas SK. A mathematical study of peristaltic transport of a Casson fluid. *Mathematical and Computer Modelling*. 2002; 35(7-8): 895-912.
- [8] Hong KS, Hong TK, Yang HS. Thermal conductivity of Fe nanofluids depending on the cluster size of nanoparticles. *Applied Physics Letters*. 2006; 88(3): 031901.
- [9] Khan WA, Pop I. Boundary-layer flow of a nanofluid past a stretching sheet. *International Journal of Heat and Mass Transfer*. 2010; 53(11-12): 2477-2483.
- [10] Warriar P, Teja A. Effect of particle size on the thermal conductivity of nanofluids containing metallic nanoparticles. *Nanoscale Research Letters*. 2011; 6(1): 1-6.
- [11] Saidur R, Leong KY, Mohammed HA. A review on applications and challenges of nanofluids. *Renewable and Sustainable Energy Reviews*. 2011; 15(3): 1646-1668.
- [12] Suresh S, Venkataraj KP, Selvakumar P, Chandrasekar M. Effect of Al₂O₃-Cu/water hybrid nanofluid in heat transfer. *Experimental Thermal and Fluid Science*. 2012; 38: 54-60.
- [13] Bhattacharyya K. Boundary layer stagnation-point flow of Casson fluid and heat transfer towards a shrinking/stretching sheet. *FHMT*. 2013; 4: 023003.
- [14] Haq RU, Nadeem S, Khan ZH, Okedayo TG. Convective heat transfer and MHD effects on Casson nanofluid flow over a shrinking sheet. *Central European Journal of Physics*. 2014; 12(12): 862-871.
- [15] Mansur S, Ishak A. Unsteady boundary layer flow and heat transfer over a stretching sheet with a convective boundary condition in a nanofluid. *American Institute of Physics*. 2014; 1614(1): 906-912.
- [16] Esfe MH, Arani AAA, Rezaie M, Yan WM, Karimipour A. Experimental determination of thermal conductivity and dynamic viscosity of Ag-MgO/water hybrid nanofluid. *International Communications in Heat and Mass Transfer*. 2015; 66: 189-195.
- [17] Harandi SS, Karimipour A, Afrand M, Akbari M, D'Orazio A. An experimental study on thermal conductivity of F-MWCNTs-Fe₃O₄/EG hybrid nanofluid: Effects of temperature and concentration. *International Communications in Heat and Mass Transfer*. 2016; 76: 171-177.
- [18] Hymavathi T, Sridhar W. Numerical solution to mass transfer in MHD flow of Casson fluid with suction and chemical reaction. *International Journal of Chemical Sciences*. 2016; 14(4): 2183-2197.
- [19] Ibrahim W, Makinde OD. Magnetohydrodynamic stagnation point flow and heat transfer of Casson nanofluid past a stretching sheet with slip and convective boundary condition. *Journal of Aerospace Engineering*. 2016; 29(2): 04015037.

- [20] Devi S, Devi S. Numerical investigation of hydromagnetic hybrid Cu-Al₂O₃/water nanofluid flow over a permeable stretching sheet with suction. *International Journal of Nonlinear Sciences and Numerical Simulation*. 2016; 17(5): 249-257.
- [21] Esfe MH, Alirezaie A, Rejvani M. An applicable study on the thermal conductivity of SWCNT-MgO hybrid nanofluid and price-performance analysis for energy management. *Applied Thermal Engineering*. 2017; 111: 1202-1210.
- [22] Ghadikolaei SS, Hosseinzadeh K, Ganji DD, Jafari B. Nonlinear thermal radiation effect on magneto Casson nanofluid flow with Joule heating effect over an inclined porous stretching sheet. *Case Studies in Thermal Engineering*. 2018; 12: 176-187.
- [23] Aman S, Zokri SM, Ismail Z, Salleh MZ, Khan I. Effect of MHD and porosity on exact solutions and flow of a hybrid Casson-nanofluid. *Journal of Advanced Research in Fluid Mechanics and Thermal Sciences*. 2018; 44(1): 131-139.
- [24] Sajid MU, Ali HM. Thermal conductivity of hybrid nanofluids: A critical review. *International Journal of Heat and Mass Transfer*. 2018; 126: 211-234.
- [25] Akhgar A, Toghraie D. An experimental study on the stability and thermal conductivity of water-ethylene glycol/TiO₂-MWCNTs hybrid nanofluid: developing a new correlation. *Powder Technology*. 2018; 338: 806-818.
- [26] Balaji Prakash G, Reddy GR, Sridhar W, Krishna YH, Mahaboob B. Thermal radiation and heat source effects on MHD casson fluid over an oscillating vertical porous plate. *Journal of Computer and Mathematical Sciences*. 2019; 10(5): 1021-1031.
- [27] Narender G, Govardhan K, Sreedhar Sarma G. MHD stagnation point Casson nanofluid flow over a radially stretching sheet. *Beilstein Archives*. 2019; 1: 137.
- [28] Sridhar W, Ganesh GR, Rao BVA, Gorfie EH. Mixed convection boundary layer flow of mhd casson fluid on an upward stretching sheet encapsulated in a porous medium with slip effects. *JP Journal of Heat and Mass Transfer*. 2021; 22(2): 133-149.
- [29] Krishna MV, Ahammad NA, Chamkha AJ. Radiative MHD flow of Casson hybrid nanofluid over an infinite exponentially accelerated vertical porous surface. *Case Studies in Thermal Engineering*. 2021; 27: 101229.
- [30] Ganesh G, Sridhar W. Numerical approach of heat and mass transfer of mhd casson fluid under radiation over an exponentially permeable stretching sheet with chemical reaction and hall effect. *Frontiers in Heat and Mass Transfer (FHMT)*. 2021; 16: 1-11.
- [31] Wang CY. Free convection on a vertical stretching surface. *ZAMM Journal of Applied Mathematics and Mechanics*. 1989; 69: 418-420.
- [32] Ganesh GR, Sridhar W. MHD radiative Casson-nanofluid stream above a nonlinear extending surface including chemical reaction through Darcy-Forchier medium. *Heat Transfer*. 2021, 50(8): 7691-7711.
- [33] Alghamdi W, Gul T, Nullah M, Rehman A, Nasir S, Saeed A, et al. Boundary layer stagnation point flow of the Casson hybrid nanofluid over an unsteady stretching surface. *AIP Advances*. 2021; 11(1): 015016.
- [34] Xu J, Wu K, Yang S, Cao J, Chen Z. Nanoscale free gas transport in shale rocks: A hard-sphere based model. *Paper presented at the SPE Unconventional Resources Conference*. 2017; 2017: D021S005R005.
- [35] Xu J, Chen Z, Wu K, Li R, Liu X, Zhan J. On the flow regime model for fast estimation of tight sandstone gas apparent permeability in high-pressure reservoirs. *Energy Sources Part A: Recovery Utilization and Environmental Effects*. 2019; 2019: 1-12.
- [36] Atashafrooz M, Sajjadi H, Amiri Delouei A. Simulation of combined convective-radiative heat transfer of hybrid nanofluid flow inside an open trapezoidal enclosure considering the magnetic force impacts. *Journal of Magnetism and Magnetic Materials*. 2023; 567: 170354.
- [37] Sajjadi H, Amiri Delouei A, Atashafrooz M. Effect of magnetic field on particle deposition in a modeled room. *Particulate Science and Technology*. 2023; 41(3): 361-370.
- [38] Delouei AA, Atashafrooz M, Sajjadi H, Karimnejad S. The thermal effects of multi-walled carbon nanotube concentration on an ultrasonic vibrating finned tube heat exchanger. *International Communications in Heat and Mass Transfer*. 2022; 135: 106098.